공학석사학위논문

Engine mount response improvement using hybrid modeling and Bayesian optimization

하이브리드 모델링과 베이지안 최적화를 이용한

엔진 마운트 응답개선

2020 년 8 월

서울대학교 대학원

기계항공공학부

강 성 호

Engine mount response improvement using hybrid modeling and Bayesian optimization

하이브리드 모델링과 베이지안 최적화를 이용한

엔진 마운트 응답개선

지도 교수 강 연 준

이 논문을 공학석사 학위논문으로 제출함

2020 년 4 월

서울대학교 대학원

기계항공공학부

강 성 호

강성호의 공학석사 학위논문을 인준함

2020 년 6 월

위 원 장 _____ (인)

부위원장 _____ (인)

위 원 _____ (인)

ABSTRACT

Engine mount response improvement using hybrid modeling and Bayesian optimization

Seong Ho Kang

Department of Mechanical and Aerospace Engineering

The Graduate School

Seoul National University

This paper presents the results of a study conducted to predict and improve the response of an engine mount using a hybrid model that combines both experimental data and finite element (FE) analysis. The engine mount is the main point of transmission of engine vibration forces to the vehicle body. Therefore, improving the dynamic response of the engine mount improves the overall NVH performance of the vehicle. The hybrid modeling method adopts the substructure synthesis method based on the frequency response function based substructuring (FBS) theory, in this method, a complex dynamic structure is divided into multiple substructures, and the frequency response function (FRF) of the entire system is predicted using the FRFs of individual substructures. This method allows engineers to predict the changes in the experimental FRF of an existing physical system by applying FE analysis only to the substructures that have undergone a design modification. The change in

the overall dynamic performance of the system can be predicted by modifying the CAD model of the substructure without preparing a physical model. Furthermore, the optimal design is proposed by applying the Bayesian optimization technique in this paper.

Keywords : Frequency Response Function (FRF), Substructure, FRF Based Substructuring (FBS), Hybrid modeling method, Engine mount, Alternator bracket, Bayesian optimization

Student Number : 2018-24764

TABLE OF CONTENTS

LIST OF TABLES

LIST OF FIGURES

CHAPTER 1

INTRODUCTION

Noise, vibration and harshness (NVH) performance in a vehicle is an important factor that enhances the quality of the vehicle and satisfaction of the customer. Numerous automobile companies worldwide have conducted several studies on the development of more accurate and effective vehicle modeling techniques to improve the NVH performance. A typical vehicle system consists of a combination of several individual substructures, such as powertrain, suspension, and body. Because of the coupling characteristics between the substructures, it is difficult to analyze the dynamic characteristics of the complex system. Hence, it is easier and more accurate to analyze the entire system by dividing it into several substructures. For this purpose, the frequency response function based substructuring (FBS) theory would be useful. This paper introduces a hybrid modeling method based on the FBS theory. According to this theory, the transfer function of the entire system can be calculated using the transfer functions of the substructures, and in the case of the hybrid modeling method, the transfer functions of the substructures are obtained from both experiments and FE analysis. It is a time-consuming process to accurately analyze the complex system, however, while analyzing only a substructure, the accuracy is high and the time required is less. The hybrid model does not require FE analysis for the entire system, but require it only for a substructure. For the substructure to which FE analysis does not apply, the

dynamic characteristics of the entire system can be using experimentally obtained results. Furthermore, the hybrid modeling method enables prediction of the effect of a design modification in the substructure performed using the FE analysis on the dynamic characteristics of the entire system. These studies can be applied in the early stages of product design, in which the design can be effectively modified to improve the NVH performance of existing products. In this paper, the focus is on improving the response level of the engine mount due to alternator vibration.

The vibrations of the engine are transmitted through the engine mounts to the body. In other words, the response of the engine mounts can be seen as the exciting force acting on the vehicle body. Thus, reducing the response of the engine mounts can reduce the vibrations transmitted to the vehicle body. In this study, the response of the engine mounts generated by alternator vibrations was is set as the target. The procedure for applying the hybrid model technique is as follows.

(1) The operational deflection shape (ODS) analysis is performed on the alternator to determine the frequency band of interest in which improvement is required.

(2) The accuracy of the hybrid model is ensured by verifying the FBS formula and comparing the results of measurements, full FE analysis, and hybrid model method.

(3) Design modification of a substructure is performed using the CAD program. (changing the structural stiffness of the alternator-bracket)

(4) The changes in engine mount response due to the changes in the structural stiffness of the alternator-bracket are analyzed in the frequency band of interest.

CHAPTER 2

LITERATURE REVIEW

(Frequency Response Function Based Sub-structuring)

2.1 Introduction

The component synthesis technique is a method of predicting the dynamic characteristics of the combined whole system from the characteristics of the individual substructure. Current component synthesis techniques include the component modal synthetics (CMS), FRF based sub-structuring (FBS), super element method, static energy analysis (SEM) and the power flow technology. For the CMS method [7-8], it is one of the ways in which theory is well organized. It has been extensively researched as a theory to synthesize the substructure using modal properties such as natural frequency, damping factor and mode shape. However, this theory requires a lot of effort and time to get experimental data as there are many modal characteristics that require measurement. It is also not suitable for analyzing the mid - frequency range NVH problems in vehicles.

For SEM and Power flow technology [9], the dynamic characteristics of the entire system are predicted through the energy flows of the substructure. These methods have the advantage of being able to analyze a wide range of frequency

bands, but they have the limitations of being difficult to predict for large systems and with sufficient information about resonances.

On the other hand, the FBS theory [1-6] is relatively convenient and can be applied to a variety of systems. It is also appropriate to apply to improving NVH problems on vehicles because of its relatively wide range of analyzable frequencies.

2.2 Frequency Response Function (FBS) theory

The two basic concepts used in the FBS theory are motion-compatibility (acceleration, Velocity, or displacement) and force equation. This concept enables the presentation of the transfer function of the entire system combined with the transfer function of the substructure only. [1-6]

For one substructure A, the transfer function matrix $[H_A]$ between displacement and force can be expressed as follows.

$$\{X_A\} = [H_A]\{F_A\} \tag{2.1}$$

$\{X_A\}$ is the response displacement vector and $\{F_A\}$ is the external excitation vector of substructure A. Substructure A coordinates have three degrees of freedom: input (i), response (o) and coupling (c). Fig. 2.1 shows three coordinates of the substructure A schematically.

Accordingly, Equation (2.1) can be divided as

$$\begin{Bmatrix}\{X\}_{o(a)}\\ \{X\}_{c(a)}\end{Bmatrix} = \begin{bmatrix}[H_A]_{o(a)i(a)} & [H_A]_{o(a)c(a)}\\ [H_A]_{c(a)i(a)} & [H_A]_{c(a)c(a)}\end{bmatrix}\begin{Bmatrix}\{F\}_{i(a)}\\ \{F\}_{c(a)}\end{Bmatrix} \quad (2.2)$$

The displacement vector, $\{X_A\}$ is divided into response and coupling coordinate $\{X\}_{o(a)}$ and $\{X\}_{c(a)}$, and the expansion vector, $\{F_A\}$ is divided into input and coupling coordinate $\{F\}_{i(a)}$ and $\{F\}_{c(a)}$. Independent substructure B combined with A can be similarly defined as

$$\{X_B\} = [H_B]\{F_B\} \quad (2.3)$$

which is divided as

$$\begin{Bmatrix}\{X\}_{o(b)}\\ \{X\}_{c(b)}\end{Bmatrix} = \begin{bmatrix}[H_B]_{o(b)i(b)} & [H_B]_{o(b)c(b)}\\ [H_B]_{c(b)i(b)} & [H_B]_{c(b)c(b)}\end{bmatrix}\begin{Bmatrix}\{F\}_{i(b)}\\ \{F\}_{c(b)}\end{Bmatrix} \quad (2.4)$$

Substructure A and B coupled systems are expressed as

$$\{X_S\} = [H_S]\{F_S\} \quad (2.5)$$

where $\{X_S\}$ and $\{F_S\}$ are coupled system displacement and force vector, and $[H_S]$ is transfer function matrix of coupled system with substructures. Since the entire system is connected by spring $[K_c]$, it can be described as Fig. 2.2, taking into account the displacement and the force relation on the coupling part.

Applying the linear system theory to each individual substructure, the coupled system response $\{X_S\}$ is caused by $\{F_S\}$ applied throughout the system and reactive forces $[R_c]$ generated at the coupling point. Considering Reactive force, response $\{Xs\}$ is expressed as

$$\{X_S\} = [H_{sub}]\{F_S\} + [H_R]\{R_c\} \tag{2.6}$$

The difference between Equation (2.5) and (2.6) is whether the coupled system response vector was expressed for the entire system or for an individual substructure. The transfer function and each vector in Equation (2.5) and (2.6) are defined as

$$[H_S] = \begin{bmatrix} [H_S]_{o(a)i(a)} & [H_S]_{o(a)c(a)} & [H_S]_{o(a)c(b)} & [H_S]_{o(a)i(b)} \\ [H_S]_{c(a)i(a)} & [H_S]_{c(a)c(a)} & [H_S]_{c(a)c(b)} & [H_S]_{c(a)i(b)} \\ [H_S]_{c(b)i(a)} & [H_S]_{c(b)c(a)} & [H_S]_{c(b)c(b)} & [H_S]_{c(b)i(b)} \\ [H_S]_{o(b)i(a)} & [H_S]_{o(b)c(a)} & [H_S]_{o(b)c(b)} & [H_S]_{o(b)i(b)} \end{bmatrix} \tag{2.7}$$

$$[H_{sub}] = \begin{bmatrix} [H_A]_{o(a)i(a)} & [H_A]_{o(a)c(a)} & [H_A]_{o(a)c(b)} & [H_A]_{o(a)i(b)} \\ [H_A]_{c(a)i(a)} & [H_A]_{c(a)c(a)} & [H_A]_{c(a)c(b)} & [H_A]_{c(a)i(b)} \\ [H_B]_{c(b)i(a)} & [H_B]_{c(b)c(a)} & [H_B]_{c(b)c(b)} & [H_B]_{c(b)i(b)} \\ [H_B]_{o(b)i(a)} & [H_B]_{o(b)c(a)} & [H_B]_{o(b)c(b)} & [H_B]_{o(b)i(b)} \end{bmatrix} \tag{2.8}$$

$$[H_R] = \begin{bmatrix} \alpha[H_A]_{o(a)c(a)} \\ \alpha[H_A]_{c(a)c(a)} \\ \beta[H_B]_{c(b)c(b)} \\ \beta[H_B]_{o(b)c(b)} \end{bmatrix} \tag{2.9}$$

$$\{X_S\} = \begin{Bmatrix} \{X\}_{o(a)} \\ \{X\}_{c(a)} \\ \{X\}_{c(b)} \\ \{X\}_{o(b)} \end{Bmatrix} \tag{2.10}$$

$$\{F_S\} = \begin{Bmatrix} \{F\}_{i(a)} \\ \{F\}_{c(a)} \\ \{F\}_{c(b)} \\ \{F\}_{i(b)} \end{Bmatrix} \tag{2.11}$$

$$\alpha = \begin{cases} +1 & \text{for} \quad X = a \\ -1 & \text{for} \quad X = b \end{cases} \tag{2.12}$$

$$\beta = \begin{cases} +1 & \text{for} \quad X = b \\ -1 & \text{for} \quad X = a \end{cases} \tag{2.13}$$

where $[H_{sub}]$ and $[H_R]$ are the substructure transfer function and $[H_S]$ is coupled system transfer function. Note that $[H_A]_{o(a)c(b)}$, $[H_A]_{o(a)i(b)}$, $[H_A]_{c(a)c(b)}$, $[H_A]_{c(a)i(b)}$, $[H_B]_{c(b)i(a)}$, $[H_A]_{c(b)c(a)}$, $[H_A]_{o(b)i(a)}$, and $[H_A]_{o(b)c(a)}$ will disappear unconditionally because the force is not transmitted between unconnected substructures. $\{R_c\}$ is the interface reactive force generated by the coupling coordinates and it divided by $\{R_{c(a)}\}$ and $\{R_{c(b)}\}$ depending on which substructure it is in. $\{R_{c(a)}\}$ and $\{R_{c(b)}\}$ are the same magnitude, but have opposite directions. That is why the sign of the transfer function $[H_R]$ in the connection coordinates depends on which substructure it is located. i.e.

$$\{R_{c(a)}\} = -\{R_{c(b)}\} \tag{2.14}$$

Applying the displacement compatibility and force equilibrium conditions, the reactive force vector at the coupling coordinates of the substructure A can be expressed as

$$\{R_{c(a)}\} = [K_c](\{X\}_{c(b)} - \{X\}_{c(a)}) \tag{2.15}$$

$\{X\}_{c(a)}$ and $\{X\}_{c(b)}$ obtained by applying Equation (2.7) -(2.14) for Equation (2.6)

$$\{X\}_{c(a)} = [H_A]_{c(a)i(a)}\{F\}_{i(a)} + [H_A]_{c(a)c(a)}\{F\}_{c(a)} + [H_A]_{c(a)c(a)}\{R_{c(a)}\} \tag{2.16}$$

$$\{X\}_{c(b)} = [H_B]_{c(b)i(b)}\{F\}_{i(b)} + [H_B]_{c(b)c(b)}\{F\}_{c(b)} - [H_B]_{c(b)c(b)}\{R_{c(a)}\}$$

(2.17)

Substituting Equation (2.16) and (2.17) into Equation (2.15),

$$\{R_{c(a)}\} = -[C]\left[[H_A]_{c(a)i(a)}[H_A]_{c(a)c(a)} - [H_B]_{c(b)c(b)} - [H_B]_{c(b)i(b)}\right]\{F_S\}$$

(2.18)

$$[C] = \left([H_A]_{c(a)c(a)} + [H_B]_{c(b)c(b)} + [K_c]^{-1}\right)^{-1} \quad (2.19)$$

Continually substitute Equation (2.19) into Equation (2.6) results in

$$\{X_S\} = [H_{sub}]\{F_S\}$$

$$-[H_R][C]\left[[H_A]_{c(a)i(a)}[H_A]_{c(a)c(a)} - [H_B]_{c(b)c(b)} - [H_B]_{c(b)i(b)}\right]\{F_S\}$$

(2.20)

Comparing Equations (2.5) and (2.20), the coupled system transfer function can be expressed only by the transfer function of the individual substructure as

$$[H_S] = [H_{sub}]$$

$$-[H_R][C]\left[[H_A]_{c(a)i(a)}[H_A]_{c(a)c(a)} - [H_B]_{c(b)c(b)} - [H_B]_{c(b)i(b)}\right]$$

(2.21)

In more specify the form, Equation (2.21) can be written as

$$\begin{bmatrix} [H_S]_{o(a)i(a)} & [H_S]_{o(a)c(a)} & [H_S]_{o(a)c(b)} & [H_S]_{o(a)i(b)} \\ [H_S]_{c(a)i(a)} & [H_S]_{c(a)c(a)} & [H_S]_{c(a)c(b)} & [H_S]_{c(a)i(b)} \\ [H_S]_{c(b)i(a)} & [H_S]_{c(b)c(a)} & [H_S]_{c(b)c(b)} & [H_S]_{c(b)i(b)} \\ [H_S]_{o(b)i(a)} & [H_S]_{o(b)c(a)} & [H_S]_{o(b)c(b)} & [H_S]_{o(b)i(b)} \end{bmatrix}$$

$$= \begin{bmatrix} [H_A]_{o(a)i(a)} & [H_A]_{o(a)c(a)} & [0] & [0] \\ [H_A]_{c(a)i(a)} & [H_A]_{c(a)c(a)} & [0] & [0] \\ [0] & [0] & [H_B]_{c(b)c(b)} & [H_B]_{c(b)i(b)} \\ [0] & [0] & [H_B]_{o(b)c(b)} & [H_B]_{o(b)i(b)} \end{bmatrix}$$

$$- \begin{bmatrix} [H_A]_{o(a)c(a)} \\ [H_A]_{c(a)c(a)} \\ -[H_B]_{c(b)c(b)} \\ -[H_B]_{o(b)c(b)} \end{bmatrix} [C] \left[[H_A]_{c(a)i(a)} [H_A]_{c(a)c(a)} - [H_B]_{c(b)c(b)} - [H_B]_{c(b)i(b)} \right]$$

(2.22)

In case where the connection of the two substructures is rigid, $[K_c]$ becomes infinite, and thus the inverse of $[K_c]$ converges into zero.

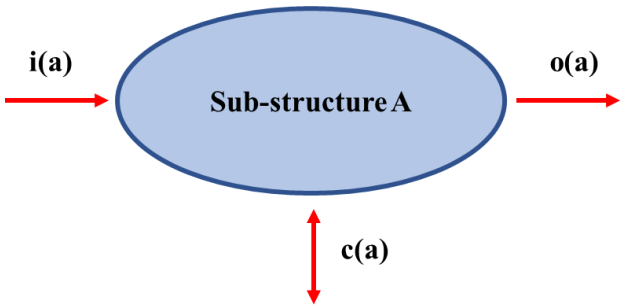

Figure 2.1 General representation of substructure

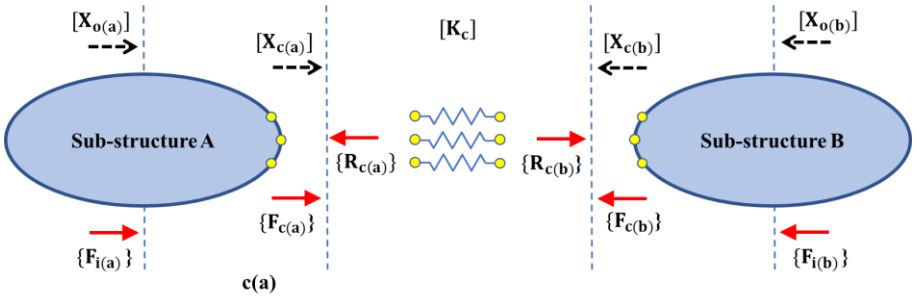

Figure 2.2 A two-substructure coupled system

CHAPTER 3

OPERATIONAL DEFLECTION SHAPE ANALYSIS

3.1 Introduction

Operational Deflection Shape (ODS) is defined as the deflection shape of a structure at a given frequency and generally refers to force induced motion at two or more points. ODS defined with a magnitude and phase value at each point on structure. At least one reference point is required for the relative magnitude and phase information of all points in order to properly define ODS vectors. ODS measurements are one of the most common analysis methods in the industry because analysis of actual movement shows how certain parts of a structure vibrates at a given frequency or if a structure is defective.[10]

3.2 ODS and waterfall analysis

Among the various parts that make up the engine, the alternator has a relatively large weight, and is connected to the engine body with a bracket. Therefore, the vibrations of the alternator are transmitted to the vehicle body

through the engine mount. To understand the movement of the alternator during actual engine operation, ODS analysis must be performed. In the experiment, the RPM of the engine is increased from 700 to 4000, and the acceleration values are recorded. Using this data, ODS and waterfall analyses are performed. Through the ODS analysis, it is confirmed that the alternator has a large movement in the Z-direction in the frequency band near 400 Hz. The Z-axis is in the direction toward the top of the engine when the engine is mounted on the vehicle. Fig. 3.1 shows the ODS of the alternator and Fig. 3.2 shows waterfall at the same point in the Z-direction. As the alternator has a resonance in the frequency band near 400 Hz, the frequency band of interest is set to, 350-500 Hz. It can be seen that the response level of the engine mount is high owing to the resonance of the alternator in the frequency band of interest. As the magnitude of acceleration of the alternator in the frequency band of interest is large, it needs to be reduced. In this study, we decided to structurally reinforce the alternator-bracket, which connects the alternator and the engine body.

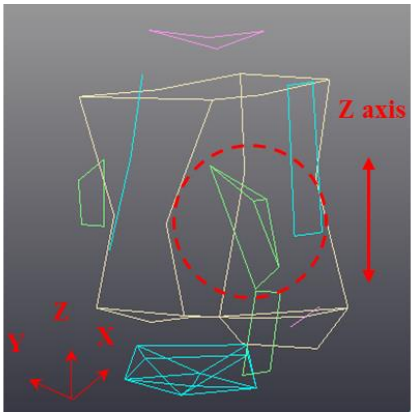

Figure 3.1 ODS of alternator

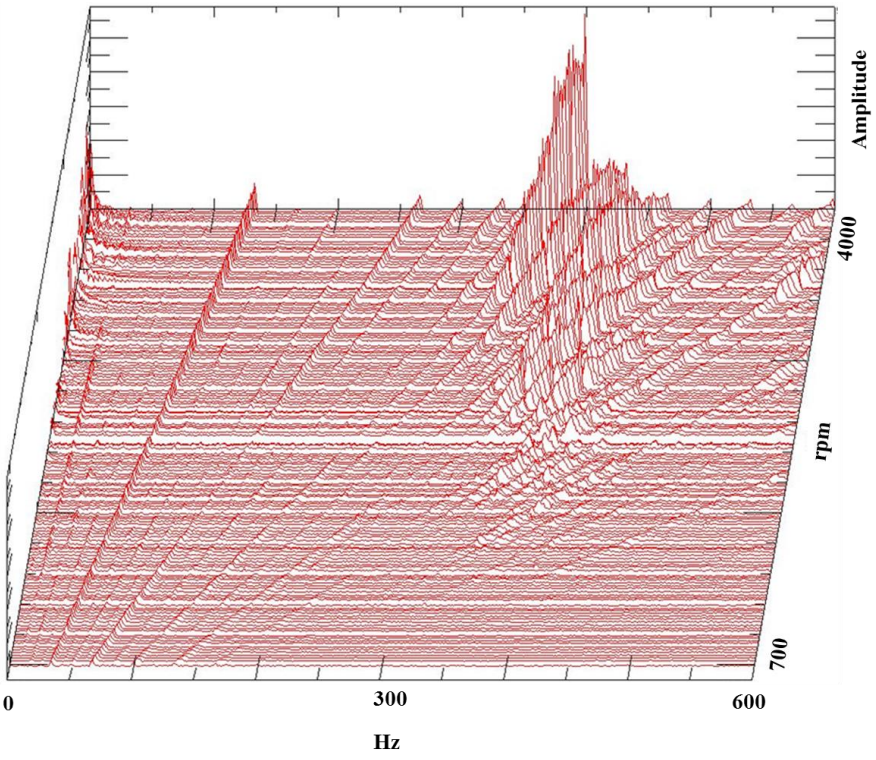

Figure 3.2 Waterfall of alternator in Z-direction

CHAPTER 4

HYBRID MODELING

4.1 Introduction

Hybrid modeling is a method that uses both Test and FE data based on the FBS theory as mentioned in Chapter 1. In this study, the model in which alternator and alternator bracket are combined is substituted into FE model, and the rest of the engine body and mount were used as actual experimental models.

Fig. 4.1 is a substructure that combines alternator and alternator bracket, which is the subject of FE analysis. Fig. 4.2 is a substructure that combines the engine body and engine mount, which is the subject of experimental analysis.

4.2 Hybrid modeling formulation

Equation (4.1) is a concise expression of only the necessary parts of the components that make up the matrix of Equation (2.22).

$$[H_S]_{o(a),i(b)} = [H_A]_{o(a),c(a)}([H_A]_{c(a),c(a)} + [H_B]_{c(b),c(b)})^{-1}[H_B]_{c(b),i(b)} \quad (4.1)$$

$[H_A]$ is the transfer function of the substructure using Test data and $[H_B]$ is the transfer function of the substructure using FE data. o(a) is the response at

the mount part, and c(a) and c(b) are the coupling points of substructures A and B, respectively. i(b) is the input point of substructure B. Note that substructure A is a system consisting of an engine mount and an engine body, and substructure B is a system consisting of an alternator and an alternator bracket.

4.3 Reliability verification of hybrid modeling method

Before using the FE analysis results for substructure B, $[H_S]_{o(a),i(b)}$ is estimated using test data for both substructures A and B to confirm that Equation (4.1) is reliable. For this equation to be reliable, the estimated $[H_S]_{o(a),i(b)}$ must be similar to the measured $[H_S]_{o(a),i(b)}$. Fig. 4.3 shows a comparison of the measured and estimated transfer functions. Both transfer functions are compared in the Z-direction. Through ODS analysis, the transfer function in the Z-axis is set as the target. It can be confirmed that although the estimated and measured transfer functions do not exactly match, they have similarities, and the response level and peak are well defined in the frequency band of interest, 350-500 Hz. Therefore, the possibility of applying the hybrid modeling method using Equation (4.1) can be confirmed.

Next, the validity of the hybrid modeling method should be confirmed. To confirm the validity, the transfer function obtained by applying the hybrid modeling method should have more similarity to the measured transfer function

compared to the result obtained by the FE analysis of the entire model. Fig. 4.4 plots $[H_S]_{o(a),i(b)}$ results obtained through measure, full-FE analysis and hybrid modeling. In the case of full FE analysis, the response level is lower than the measured transfer function in the frequency band of interest and the peak is not well defined. On the other hand, in the case of the results obtained using the hybrid modeling method, the graph is relatively well defined. Table 4.1 presents a comparison of the time required to calculate $[H_S]_{o(a),i(b)}$ by using the full FE analysis and the hybrid modeling method. It can be seen from Fig. 4.4 that the hybrid modeling method has more similarity to the experimental data than the full FE analysis. The reason for this result is that the numerical analysis is performed on the entire system in the full FE analysis, but in the hybrid modeling method, experimental data are used for the substructures. In the case of the hybrid modeling method, because the FE analysis is performed only on some substructures compared to the full FE analysis, the time required for calculation is drastically reduced.

4.4 Alternator bracket design modification

Having confirmed the usefulness of hybrid modeling, the design of the substructure is modified and the transfer function [Hs] is predicted. The subject of design modification is the alternator-bracket, which is the part connecting the alternator and the engine body. The design modification is aimed at suppressing the movement in the Z-axis in the frequency band of interest, 350-500 Hz. To suppress this movement, nine rods are added to the alternator-bracket to increase the structural stiffness. Five cases with change in the cross-sectional area of the rod, in both aluminum alloy and steel, are considered, the diameter is increased in steps of 2.5 mm, from 5 mm to 15 mm. Using the hybrid modeling method, it is possible to predict the change in the response of the engine mount with the structural stiffness modification of the alternator-bracket. Fig. 4.5 shows the original and modified alternator brackets.

Table 4.2 presents material property of each rod and Table 4.3 presents the overall response level at 350-500 Hz when applying aluminum rod for increase structural stiffness of alternator-bracket. As shown in Table 4.3, when the rod diameter is 12.5 and 15 mm, the overall response level is effectively reduced. Fig 4.6~10 show the comparison of the measured, hybrid modeling $[H_S]_{o(a),i(b)}$ for the original bracket and hybrid modeling $[H_S]_{o(a),i(b)}$ for the modified bracket when using aluminum alloy rod (5, 7.5, 10, 12.5 and 15 mm diameter).

Table 4.4 shows the overall response level at 350-500 Hz when applying steel rod for increase structural stiffness of alternator-bracket. The Young's modulus of steel is about 3 times larger than aluminum alloy. Therefore, when an aluminum alloy rod is used, the overall response level of the engine mount is reduced more effectively. Fig 4.11~15 show the comparison of measured, hybrid modeling $[H_S]_{o(a),i(b)}$ for the original bracket and hybrid modeling $[H_S]_{o(a),i(b)}$ for the modified bracket when using steel rod (5, 7.5, 10, 12.5 and 15 mm diameter).

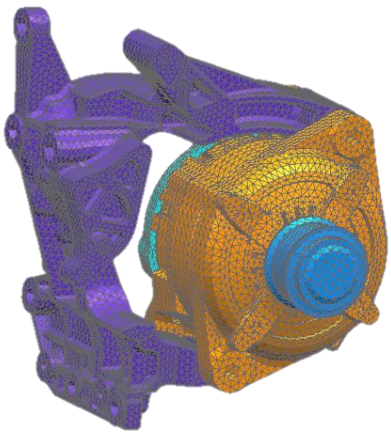

Figure 4.1 Alternator and alternator bracket assembly system (Subject to FE analysis)

Figure 4.2 Engine body and engine mount assembly system (Subject to experimental analysis)

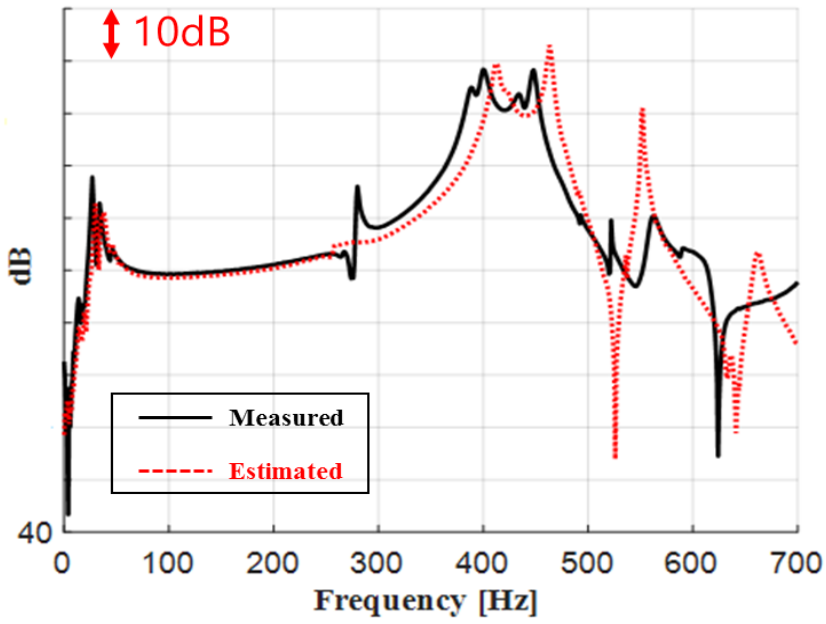

Figure 4.3 Comparison of measured and estimated $[H_S]_{o(a),i(b)}$ in Z direction of the engine

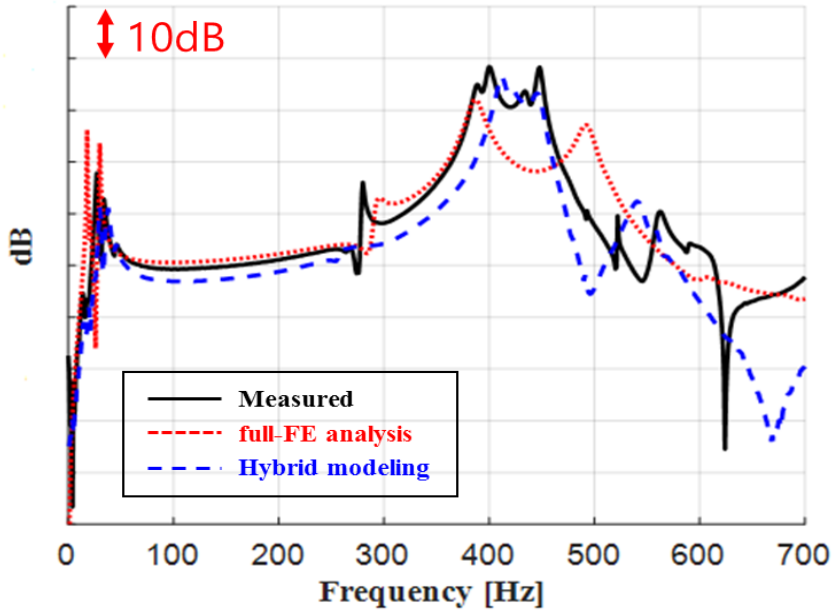

Figure 4.4 Comparison of measured, full-FE analysis and hybrid modeling $[H_S]_{o(a),i(b)}$ in Z direction of the engine

Table 4.1 Time required to calculate $[\mathbf{H_S}]_{\mathbf{o(a),i(b)}}$ for each method

Method	Time required
Full-FE	11 h
Hybrid	5 min

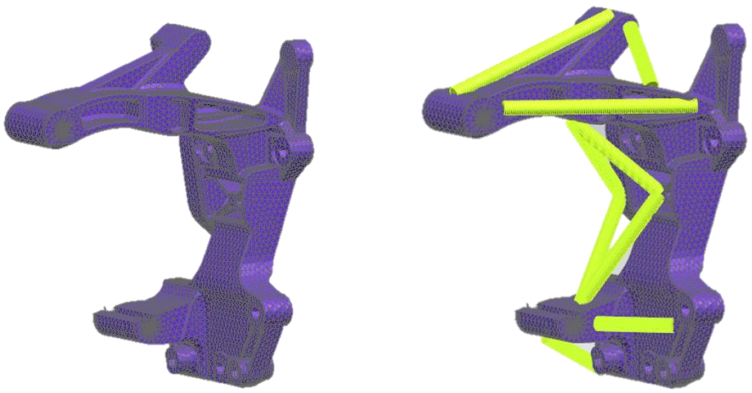

Figure 4.5 Original alternator bracket (left) and Modified alternator bracket (right)

Table 4.2 Material property of each rod

Rod type	Yong's modulus $[GPa]$	Poisson's ratio	Structure damping Coefficient	Mass density $[kg/mm^3]$
Aluminum Alloy	71	0.33	0.03	$2.7e-06$
Steel	210	0.29	0.02	7.9e-06

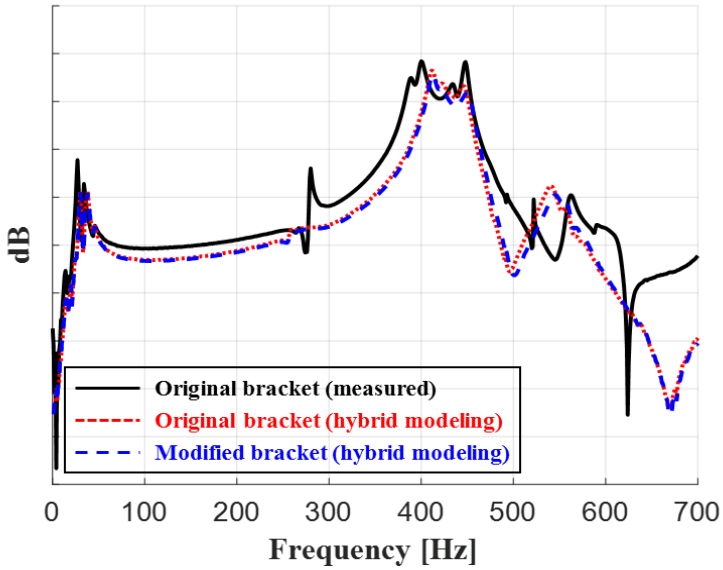

Figure 4.6 Comparison of measured, full-FE analysis and hybrid modeling $[H_S]_{o(a),i(b)}$ in Z direction of the engine (using 5mm diameter aluminum alloy rod)

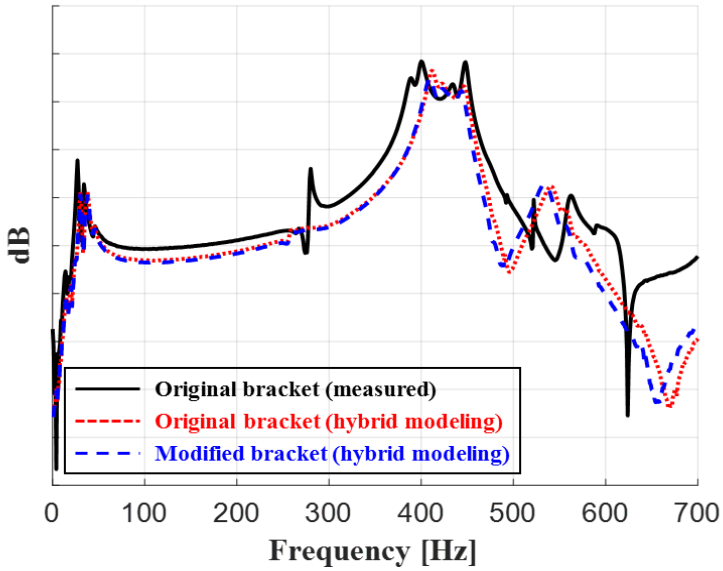

Figure 4.7 Comparison of measured, full-FE analysis and hybrid modeling $[H_S]_{o(a),i(b)}$ in Z direction of the engine (using 7.5mm diameter aluminum alloy rod)

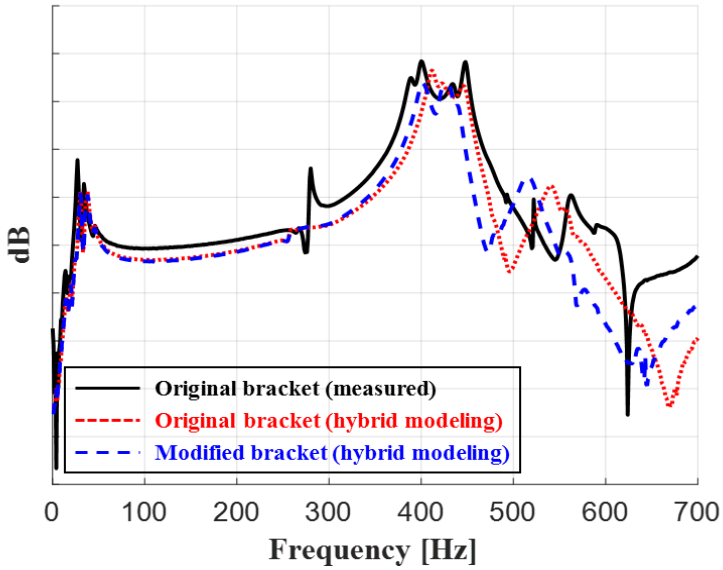

Figure 4.8 Comparison of measured, full-FE analysis and hybrid modeling $[H_S]_{o(a),i(b)}$ in Z direction of the engine (using 10mm diameter aluminum alloy rod)

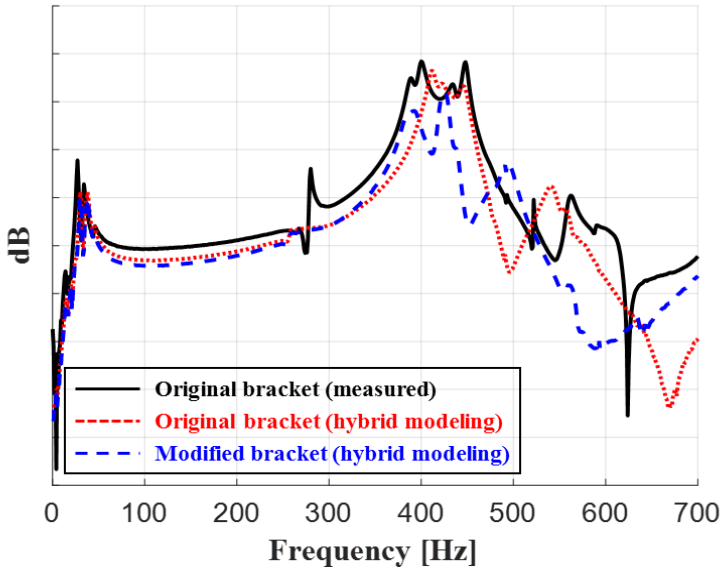

Figure 4.9 Comparison of measured, full-FE analysis and hybrid- modeling $[H_S]_{o(a),i(b)}$ in Z direction of the engine (using 12.5mm diameter aluminum alloy rod)

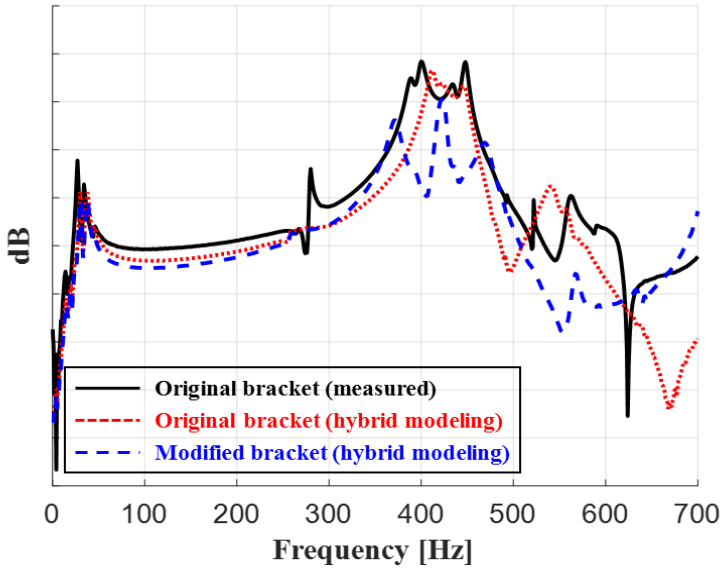

Figure 4.10 Comparison of measured, full-FE analysis and hybrid- modeling $[H_S]_{o(a),i(b)}$ in Z direction of the engine (using 15mm diameter aluminum alloy rod)

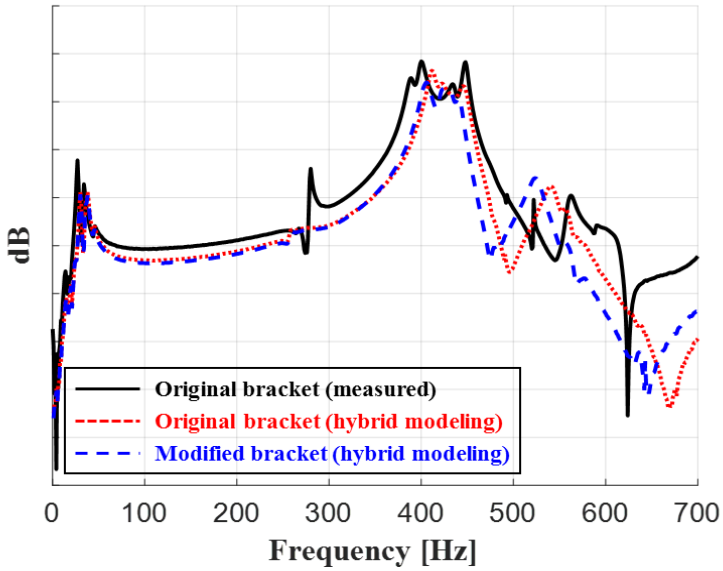

Figure 4.11 Comparison of measured, full-FE analysis and hybrid- modeling $[H_S]_{o(a),i(b)}$ in Z direction of the engine (using 5mm diameter steel rod)

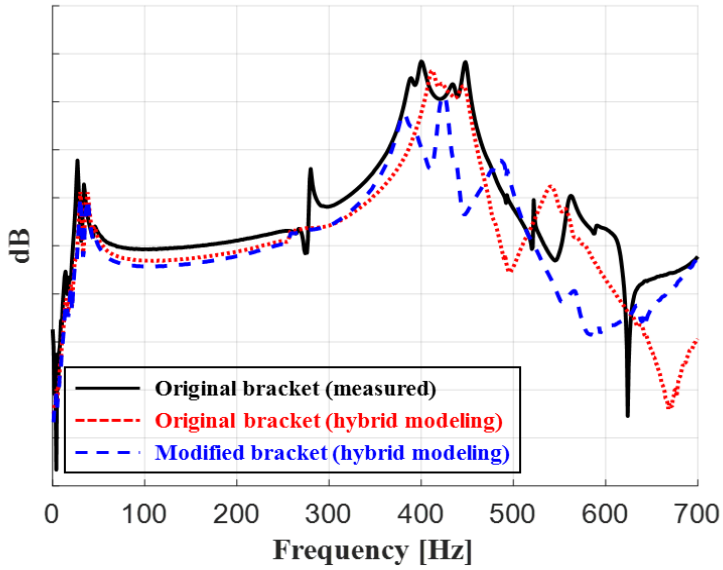

Figure 4. 12 Comparison of measured, full-FE analysis and hybrid modeling $[H_S]_{o(a),i(b)}$ in Z direction of the engine (using 7.5mm diameter steel rod)

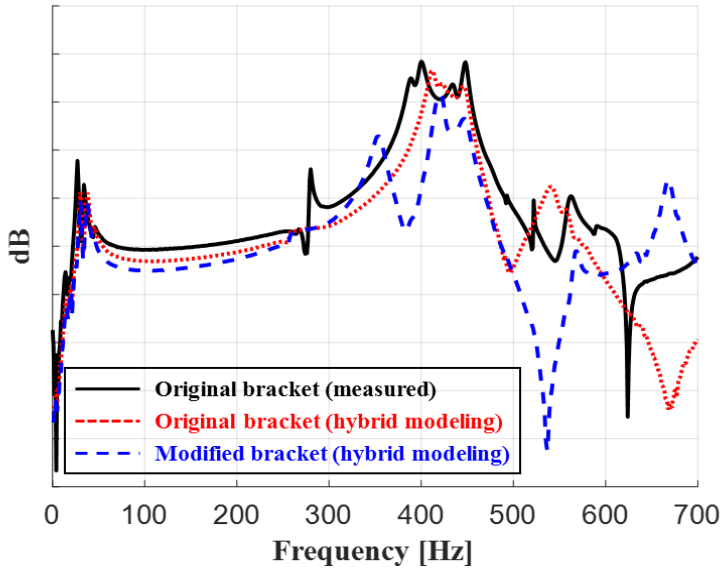

Figure 4.13 Comparison of measured, full-FE analysis and hybrid modeling $[H_S]_{o(a),i(b)}$ in Z direction of the engine (using 10mm diameter steel rod)

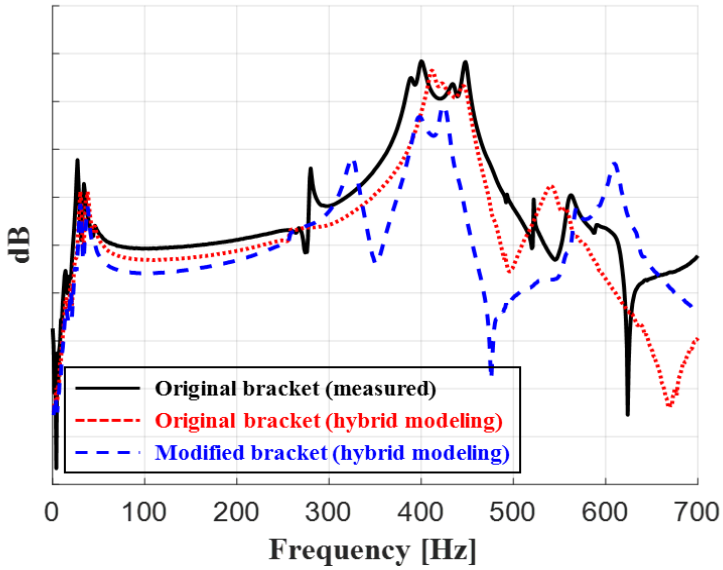

Figure 4.14 Comparison of measured, full-FE analysis and hybrid modeling $[H_S]_{o(a),i(b)}$ in Z direction of the engine (using 12.5mm diameter steel rod)

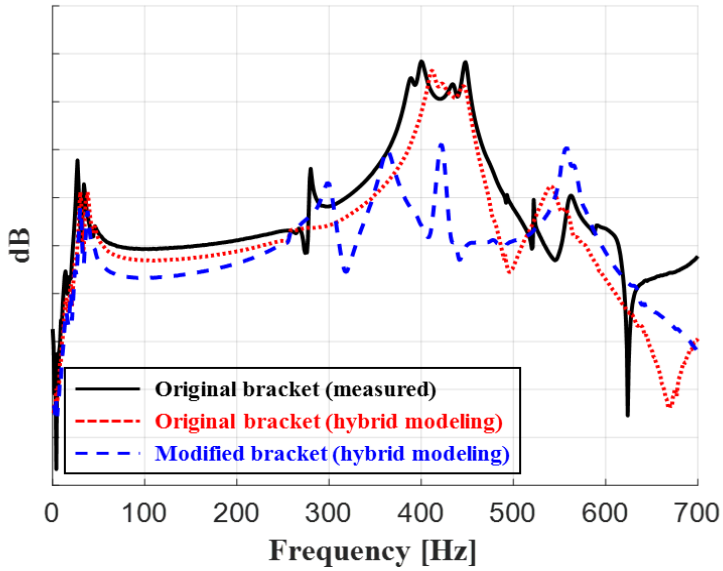

Figure 4.15 Comparison of measured, full-FE analysis and hybrid modeling $[H_S]_{o(a),i(b)}$ in Z direction of the engine (using 15mm diameter steel rod)

Table 4.3 Comparison of the overall response level of $[H_S]_{o(a),i(b)}$ when using an original bracket and modified by aluminum alloy rod (350 to 500 Hz)

Diameter [*mm*]	Overall response level of modified bracket [dB]	Overall response level of original bracket [dB]
5	109.8	109.8
7.5	108.4	
10	108.2	
12.5	107.9	
15	107.4	

Table 4.4 Comparison of the overall response level of $[H_S]_{o(a),i(b)}$ when using an original bracket and modified by steel rod (350 to 500Hz)

Diameter [*mm*]	Overall response level of modified bracket [dB]	Overall response level of original bracket [dB]
5	107.8	109.8
7.5	107.9	
10	104.7	
12.5	97.0	
15	96.4	

CHAPTER 5

BAYESIAN OPTIMAIZATION

5.1 Bayesian optimization theory

Bayesian optimization is an algorithm that searches the optimal parameters of a given model through an artificial intelligence sampling process. In particular, it is easy to solve the problem of black-box optimization, which is difficult to express mathematically without knowing the objective function. Recently, it has been spotlighted because it can effectively tune the hyperparameters of various deep learning algorithms [13]. The key idea of Bayesian optimization is to find the optimal value with minimal exploration using the surrogate model. Surrogate model is a model that stochastically estimates an unknown objective function based on observed values from the past to the present. In this study, Bayesian linear regression model was used as in Equation (5.1).

$$y = \boldsymbol{w}^{\mathrm{T}}\phi(\boldsymbol{x}) + \epsilon \ , \tag{5.1}$$

where, $\boldsymbol{x} \in \Re^d$ is a vector of input, $\phi: \Re^d \to \Re^l$ is a random feature map, $\boldsymbol{w} \in \Re^l$ is a vector of weight and ϵ is noise corresponding $\mathcal{N}(0, \sigma^2)$. The random feature map is defined such that the inner product corresponds to the

Gaussian kernel [14] as in Equation (5.2).

$$\phi(\boldsymbol{x})^{\mathrm{T}}\phi(\boldsymbol{x}') = \exp\left(-\frac{\|\boldsymbol{x}-\boldsymbol{x}'\|^2}{\eta^2}\right) . \quad (5.2)$$

The acquisition function must be defined in order to locate the optimal point through the surrogate model. Also, for global optimization, exploitation and exploration must be properly balanced. In this study, the expected improvement (EI) [15] defined in Equation (5.3) was used.

$$\mathrm{EI}(\boldsymbol{x}) = \mathbb{E}[max(f(\boldsymbol{x}) - f(\boldsymbol{x}^+), 0)] . \quad (5.3)$$

where, $f(\boldsymbol{x}^+)$ means the maximum function value among the observed values from the past to the present. The Acquisition function using EI estimates a location where there is a high probability that an optimal point exists based on data searched from the past to the present. The surrogate model is updated through observation of the point. After this iterative learning process, Bayesian optimization can effectively find the global optimum value of the black-box function.

5.2 Optimization of structural stiffness of alternator bracket using Bayesian optimization

If the structural rigidity of the bracket is changed using the nine rods in Chapter 4, it has disadvantageous in terms of weight and cost. Therefore, the Bayesian optimization technique was used to reduce engine mount response efficiently with a small number of rods. Assuming that any of the 9 rods is

selected, the number of 126 cases (No. 1-126) is possible. Since it takes too much time to perform all of these cases, the Bayesian optimization technique was used to find the most efficient case while verifying the minimum number of cases. After training the surrogate model with the first 5 random cases as inputs, the next 5 cases are recommended through the acquisition function. Repeat the same learning process with the response level of the five recommended cases as input again. Fig. 5.2.1 shows that the case with the lowest response level was found by repeating the 5 learnings starting with the 5 random cases initially set. The required number of verification data is about 20% out of 126 (25 cases). Fig. 5.2.2 is the result of learning by setting random cases to be used as input (random input 2) different from random input 1. Compared to Random input 1, the optimal case was found only by verifying 20 cases, which is about 16% of the total number of cases. For verification of the optimal case (No.12) with 104.7 dB, all 126 cases were confirmed through hybrid modeling techniques, and as a result, No.12 case was confirmed that the optimal case with the lowest response level. Fig. 3.2.3 describes the rod position of No.12, the optimal case.

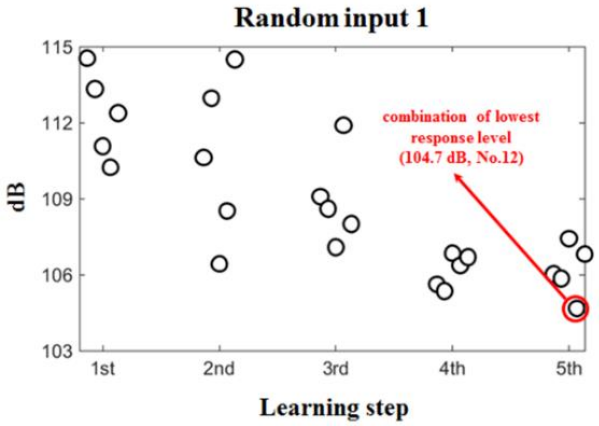

Figure 5.1 Learning steps to find the optimal case (using random input 1)

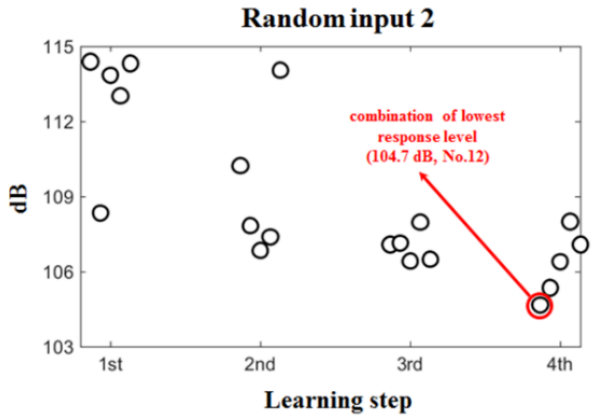

Figure 5.2 Learning steps to find the optimal case (using random input 2)

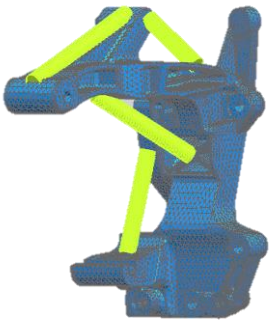

Figure 5.3 Optimal modified bracket (No.12)

CHAPTER 6

CONCLUSION

6.1 Contribution

The hybrid modeling method contains experimental data, so its accuracy is higher than the full-FE analysis. In addition, it has the advantage that it can quickly predict how the transfer function will change for the part that needs to be modified in design without further experiment. This can be useful in solving the vehicle NVH problem in the preceding stage of the automobile development stage. Based on the FBS theory, this method predicts the transfer function of the entire system through the FE analysis of only the substructure that require partial design modify with the FE model. Subsequently, it is possible to predict the change of the transfer function of the entire system through simple design modification through a computer of the substructure to which FE analysis is applied. In this study, the hybrid modeling method is used to reduce the engine mount response due to alternator vibration. Structural problems of the alternator bracket were identified through ODS analysis. In order to improve structural problems, the structural stiffness is increased by adding a rod made of aluminum alloy and steel in the CAD model of alternator bracket. As a result, it was possible to reduce the engine mount response in the frequency band of

interest. Through this concept, the direction of design modification can be suggested without additional experiments on the object that needs a design modification in the actual vehicle development stage, which will drastically reduce the time and cost of the automobile development stage [12-13]. In addition, since it can obtain a lot of data quickly, it can be applied to artificial intelligence (AI) learning such as machine learning and deep learning.

6.2 Future work

Although the hybrid modeling method is effective in predicting the transfer function of the entire system where design modification have been made, it does not exactly match the transfer function obtained in the experiment. Due to these problems, several future research is proposed for the hybrid modeling method.

(1) In this study, it was assumed that when applying the FBS theory, independent coupling was performed without affecting between perfectly coupled points. However, in fact, when the alternator bracket is combined with the engine body, it is estimated that there will be some influence between the coupled points, and for accurate results, it is necessary to consider all cross terms between coupling points. The contents related to this are presented in more detail in Reference [6].

(2) The hybrid modeling method is more accurate than full-FE analysis because FE analysis is applied only to the substructure, but errors are

inevitable because FE analysis is performed anyway. To overcome this, it is recommended to perform correlation evaluation between test data and FEM data between substructures.

REFERENCES

[1] TSAI, J.-S.; CHOU, Y.-F. The identification of dynamic characteristics of a single bolt joint. *Journal of Sound and Vibration*, 1988, 125.3: 487-502.

[2] REN, Y.; BEARDS, C. F. On substructure synthesis with FRF data. *Journal of Sound and Vibration*, 1995, 185.5: 845-866.

[3] VOORMEEREN, S. N.; RIXEN, D. J. A family of substructure decoupling techniques based on a dual assembly approach. *Mechanical Systems and Signal Processing*, 2012, 27: 379-396.

[4] NICGORSKI, Dana; AVITABILE, Peter. Conditioning of FRF measurements for use with frequency based substructuring. *Mechanical Systems and Signal Processing*, 2010, 24.2: 340-351.

[5] GUO, Rong, et al. Numerical investigation of a two-stage serial vibration isolation system using frequency response function based substructuring method. *Advances in Mechanical Engineering*, 2017, 9.4: 1687814017696654.

[6] LIU, Lei. A frequency response function-based inverse substructuring approach for analyzing vehicle system NVH response. 2003.

[7] KUANG, J. H.; TSUEI, Y. G. A more general method of substructure mode synthesis for dynamic analysis. *AIAA journal*, 1985, 23.4: 618-623.

[8] HINTZ, Robert Morris. Analytical methods in component modal synthesis. *AIAA Journal*, 1975, 13.8: 1007-1016.

[9] HYNNA, P.; KLINGE, Paul; VUOKSINEN, Jukka. Prediction of structure-borne sound transmission in large welded ship structures using statistical energy analysis. *Journal of sound and vibration*, 1995, 180.4: 583-607.

[10] JIN, Si; PAI, P. Frank. Locating structural defects using operational deflection shapes. *Journal of intelligent material systems and structures*, 2000, 11.8: 613-630.

[11] LIU, Lei; LIM, Teik C. Application of FRF-based inverse substructuring analysis to vehicle NVH problems. *SAE transactions*, 2003, 2006-2012.

[12] CUPPENS, K.; SAS, Paul; HERMANS, L. Evaluation of the FRF based substructuring and modal synthesis technique applied to vehicle FE data. In: *Proceedings of the International Seminar on Modal Analysis*. KU Leuven; 1998, 2001, 1143-1150.

[13] Snoek, J., Larochelle, H., & Adams, R. P., Practical bayesian optimization of machine learning algorithms. In *Advances in neural information processing systems*,2012, 2951-2959.

[14] Rahimi, A., & Recht, B., Random features for large-scale kernel machines. In *Advances in neural information processing systems*, 2008, 1177-1184.

[15] Jones, D. R., Schonlau, M., & Welch, W. J., Efficient global optimization of expensive black-box functions. *Journal of Global optimization*, *13*(4), 1998, 455-492.

국문 초록

본 논문에서는 차량 엔진 구조물에 대해 실험 데이터와 유한요소 해석 데이터를 모두 이용하는 Hybrid 모델의 부분구조합성법을 통해 엔진 마운트에서의 응답을 예측하는 연구를 수행하였다. Hybrid 모델 부분구조 합성법은 복잡한 전체 시스템을 여러 개의 부분구조로 나누어 각각의 Frequency Response Function(FRF)만으로 전체 시스템의 FRF 를 예측하는 FRF Based Sub-structuring(FBS)이론을 기반으로 하며, 특정 부분 구조물은 실험 데이터를 다른 부분 구조물은 유한요소해석 데이터를 사용한다. 이러한 방법은 시스템 일부분의 변화가 시스템 전체에 미치는 영향을 빠르게 파악 할 수 있기 때문에 여러 분야에서 활발하게 연구하고 적용되고 있다. 특히, 제품이 개발된 후 성능개선을 위한 부분 구조물의 설계변경에 따른 전체 시스템의 FRF 를 예측하는 데 유용하게 사용된다. 일반적으로 설계변경이 이뤄지는 부분 구조물의 경우 유한요소해석 데이터를 사용하는데 이는 실험 데이터와 달리 실제 물리적 모델 제작 없이 컴퓨터를 이용한 간단한 모델링 변경만으로도 전체 시스템의 성능을 예측할 수 있기 때문이다. 본 연구에서는 엔진 마운트의 응답을 예측하고 감소시키기 위해 Hybrid 모델의 부분구조합성법이 적용되었다.

엔진 마운트의 경우 그 응답이 차체로 유입되는 가진력이 되므로 차량 전체의 NVH 성능 개선을 위해선 엔진 마운트의 응답 레벨을 줄이는 것이 필요하다. 유한요소해석이 적용되는 알터네이터 브라켓의 구조변경에 따라 엔진 마운트 응답이 어떻게 달라지는지 예측하고 이러한 경향성을 통해 엔진 마운트 응답을 줄이는 방안을 제시한다. 더 나아가 Hybrid 모델링 기법을 통해 많은 데이터를 빠르게 얻을 수 있다는 장점을 활용하여, Bayesian optimization 기법을 적용하였고 이를 통해 알터네이터 브라켓의 최적화된 구조강성을 도출하였다.

주요어 : 주파수응답함수, 부분구조물, 주파수응답함수를 이용한 부분구조 합성법, 혼합 부분구조 합성법, 엔진마운트, 알터네이터 브라켓, 베이지안 최적화

학 번 : 2018-24764